Materials Research Letters

ISSN: 2166-3831 (Online) Journal homepage: www.tandfonline.com/journals/tmrl20

Mechanical Behavior of Micronanoscaled Metallic Glasses

Lin Tian, Xiao-Lei Wang & Zhi-Wei Shan

To cite this article: Lin Tian, Xiao-Lei Wang & Zhi-Wei Shan (2016) Mechanical Behavior of Micronanoscaled Metallic Glasses, Materials Research Letters, 4:2, 63-74, DOI: 10.1080/21663831.2015.1124298

To link to this article: https://doi.org/10.1080/21663831.2015.1124298

© 2016 The Author(s). Published by Taylor & Francis.

Published online: 22 Jan 2016.

Submit your article to this journal

Article views: 3185

View related articles

View Crossmark data

Citing articles: 7 View citing articles

Full Terms & Conditions of access and use can be found at
https://www.tandfonline.com/action/journalInformation?journalCode=tmrl20

MATERIALS RESEARCH LETTERS

Mater. Res. Lett., 2016
Vol. 4, No. 2, 63–74, http://dx.doi.org/10.1080/21663831.2015.1124298

Taylor & Francis
Taylor & Francis Group

www.tandfonline.com/toc/tmrl20/current

Mechanical Behavior of Micronanoscaled Metallic Glasses

Lin Tian*, Xiao-Lei Wang and Zhi-Wei Shan*

Center for Advancing Materials Performance from the Nanoscale (CAMP-Nano) & Hysitron Applied Research Center in China (HARCC), State Key Laboratory for Mechanical Behavior of Materials, Xi'an Jiaotong University, Xi'an, People's Republic of China

(*Received 3 October 2015; final form 20 November 2015*)

In this paper, research on the mechanical behavior of micronanoscaled metallic glasses (MGs) is reviewed, with an emphasis on works achieved through *in situ* transmission electron microscope. It was found that the strength of micronanoscaled MGs has a nonlinear dependence on sample size. Corresponding to the transition of size-dependent strength, the deformation mechanism of MGs changes gradually from brittle to ductile with the critical transition size being affected by strain rate, e-beam irradiation and thermal history of the sample. Besides monotonic loading, the mechanical behaviors of MGs in response to cyclic loadings and fatigue tests are also reviewed.

Keywords: Metallic Glasses, Micronanoscaled, Plasticity, Strength, Cyclic Loading

Introduction Metallic glasses (MGs), also known as amorphous metals, are materials composed of metal components but without crystalline structure.[1–3] The lack of long–range order, that is, atoms do not register in periodic lattice sites, renders MGs unique in mechanical behaviors.[4–7] Unlike crystalline metals, MGs do not have dislocation or deformation twinning as plastic carriers. When the applied mechanical load exceeds their yield strength, bulk MGs usually deform through the formation of shear band, a thin band where large shear strains localized [8], usually in a catastrophic manner. The stress level required for the nucleation and propagation of shear band is much higher than that for dislocations or twins in bulk crystalline materials, usually on the GPa level. Without early yielding, the measured elastic limit for bulk MGs can be up to 2% [4,9], much larger than their crystalline counterparts. Even though the brittleness and high cost limit the commercialization of bulk MGs, recent studies [10–12] demonstrated that micronanoscaled (refer to samples with their size ranged from 10 nm to 10 μm [13]) MGs own outstanding strength and reasonable plastic deformability which make them attractive for applications in Micro/Nano electro-mechanical systems (M/NEMS). Consequently, a systematic study of the mechanical properties of micronanoscaled MGs is of great industrial importance and academic interest.

In this paper, the major progress achieved in the past decade on probing the mechanical behavior of micronanoscaled MGs will be reviewed. The first section focuses on the size dependence of strength and the following section discusses the size dependence of plastic deformation mechanism. The third section summarizes the results on fatigue properties. And the last section discusses the potential artifacts from the experimental setup. These results not only revealed interesting mechanical behavior of micronanoscaled MGs but also shed new lights on the understanding of the deformation mechanism in MGs. The established quantitative mechanical data suggested that MGs are promising candidates for structural materials in M/NEMS applications.

Strength–Size Relationship In 2005, Volkert et al. [14] reported the effect of sample size on the deformation behavior of $Pd_{77}Si_{23}$ MG. The experimental setup is shown in Figure 1. Pillar samples with their diameters ranging from 140 nm to 8 μm were fabricated using Focused Ion Beam (FIB) and compressed using a nanoindentation system equipped with a flat diamond punch.

*Corresponding authors. Email: lintian@xjtu.edu.cn, zwshan@xjtu.edu.cn

© 2016 The Author(s). Published by Taylor & Francis.
This is an Open Access article distributed under the terms of the Creative Commons Attribution License (http://creativecommons.org/Licenses/by/4.0/), which permits unrestricted use, distribution, and reproduction in any medium, provided the original work is properly cited.

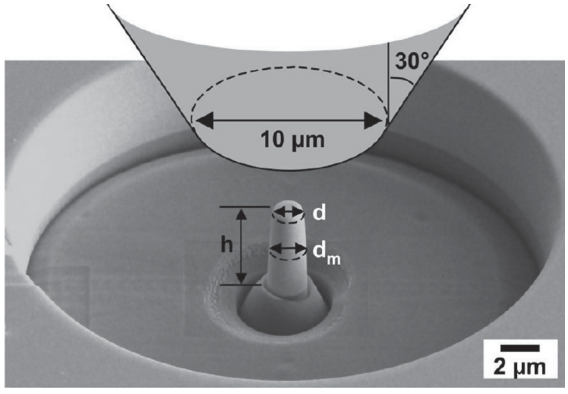

Figure 1. SEM image of a 2 μm diameter column and schematic of the punch used for compression testing.[14]

As shown in Figure 2(a), they found that the flow stresses at 5% plastic strain increase slightly with the decreasing sample diameter in the size range from 400 nm to 8 μm (The strength and deformation mechanism of samples smaller than 400 nm will be discussed in the next section). This strength–size relationship was proposed to result from an energy-balance model [14–19], that is, the strain energy relief during yielding is consumed by the creation of the shear band. Following this seminal work, 'size effect' on the strength of a wide range of MGs was investigated. As shown in Table 1, even though the majority of the researchers reported that sample size did affect the strength of MGs (e.g. Figure 2(b) [20]), there are several works which claimed that no such trend was found in their tests (e.g. Figure 2(c) [21]). In order to resolve this dispute, Wang et al. [22] carried out a systematic study on $Al_{88}Fe_7Gd_5$ MG by employing *in situ* compression tests on pillars in both Scanning Electron Microscope (SEM) and Transmission Electron Microscope (TEM) and *in situ* uniaxial tensile tests inside TEM. They demonstrated that when the sample size falls in between 100 nm to a few micron meters, $Al_{88}Fe_7Gd_5$ MG does exhibit obvious size strengthening behavior. In view of their experiment data, Wang et al. [22] proposed a shifted-$D^{-0.5}$ power law dependence of strength with decreasing sample diameter based on a modified energy-balance model to explain the stress–size relationship. The actual elastic energy release during the load drop caused by the propagation of shear band instead of total energy stored in the sample is used in this model. It was interesting to note that the resulting simple power law fits other published strength data for a number of MG systems, too (see Figure 3 [22]).

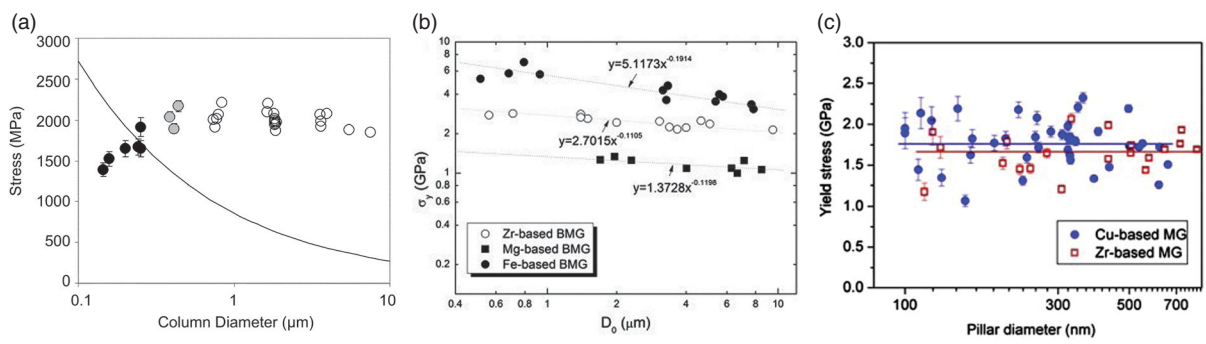

Figure 2. (Colour online) Stress–size relationship of different MGs. (a), (b) and (c) are reproduced from references [14], [20], and [21] respectively.

Table 1. Size effects in MGs.

References	Composition	Loading	Strength size dependence	Tested size range
Volkert et al. [20]	$Pd_{77}Si_{23}$	Compression	Dependence	140 nm – 8 μm
Schuster et al. [23,24]	$Pd_{40}Ni_{40}P_{20}$	Compression	Dependence	250 nm – 20 μm
Wang et al. [25]	$Pd_{40}Cu_{30}Ni_{10}P_{20}$	Tension	Dependence	340 nm – 1.2 μm
Wang et al. [22]	$Al_{88}Fe_7Gd_5$	Compression	Dependence	170 nm – 3 μm
Lai et al. [26]	Zr-based	Compression	Dependence	0.7, 1 and 3.8 μm
Jang et al. [15] [10]	Zr-based	Compression Tension	Dependence	100 nm – 1.6 μm
Bharathula et al. [27,28]	Zr-based	Compression	Dependence	200 nm – 3.6 μm
Ye et al. [20]	Zr-based Mg-based Fe-based	Compression	Dependence	500 nm – 10 μm
Dubach et al. [17]	Zr-based	Compression	Independence	0.3, 1 and 3 μm
Kuzmin et al. [29]	Zr-based	Compression	Independence	90 nm – 600 nm
Chen et al. [21] [30]	Cu-based	Compression	Independence	70 nm – 645 nm
Kuzmin et al. [31,32]	Al-based	Compression	Independence	110 nm – 900 nm

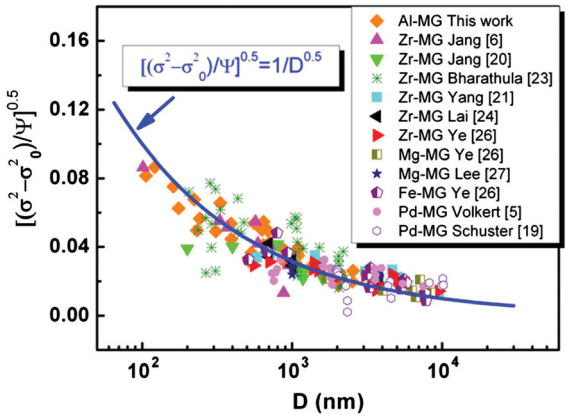

Figure 3. (Colour online) A general model (based on shear band initiation) is used to fit the experiment data and other published data for size-dependent strength in various MG at the micro- and nanoscale, giving a shifted-$D^{-0.5}$ dependence. The literature strength data used in this plot are all for samples that exhibited shear banding as the controlling mode for yielding.[22]

Compared to crystalline materials, MGs have superior elastic limit.[33] If MGs indeed have size strengthening, one reasonable speculation is that much higher elastic strain should be measured in micronanoscaled samples, as predicted by the theoretical prediction.[34] The micronanoscaled materials offer opportunities to explore the elastic limit of MGs in experiment. However, compression tests are not suitable for the study of elastic behavior of MGs due to the imperfections of the experiment setup. First of all, the pillars fabricated through FIB usually have a tapered geometry, and round tops instead of flat tops are always found for pillars with smaller size. The tapered geometry and the round tops will undoubtedly generate stress gradient and therefore strain localization (sometimes causing a mushroom geometry [35]). All these geometry complications make it difficult to ascertain the actual deformation stresses and their distributions, which also significantly deviate from the presumed uniaxial stress condition. Second, the inevitable contact interface between the compressing punch and the pillar sample often serves as the site for heterogeneous nucleation of shear bands, resulting in lower nominal stresses for yielding and data scattering. Third, the friction and confinement applied by the punch to the tested pillars can also affect the observed deformation mode and the stress required to activate it.[10] In order to rule out these experimental artifacts, there is a pressing need to use *in situ* quantitative uniaxial tension technique, which is a simple and informative method to reveal the fundamental mechanical properties such as elasticity, yield/flow stress and ductility even though it is much more challenging to carry out in practice for micronanoscaled samples.

Jang and Greer [15] was the first to report results of *in situ* quantitative SEM tensile tests of micronanoscaled MGs. The typical sample geometry used in their study is shown in Figure 4(a). For the samples with their diameter ranging from 1000 nm to about 500 nm, a weak size strengthening trend can be identified (Figure 4(b)). However, little attention has been paid to the stress or strain limit achieved in their tests, perhaps due to the slight taper in their sample design. In order to reveal if theoretical high stress or elastic strain limit can be achieved experimentally, Tian et al. [11] carried out *in situ* quantitative TEM tensile tests on $Cu_{49}Zr_{51}$ MG. Different from previous tests, the samples were carefully designed to achieve the following goals. First, minimize or even eliminate the stress concentration. Geometrically, this goal was achieved through finite-element-analysis-assisted sample design and the following very careful fabrication procedure; microstructurally, the sample size was controlled to be in the range of 200–300 nm to minimize the chance to contain growth flaws. Second, measure the strain in the gauge part precisely. This was the most challenging part for the uniaxial

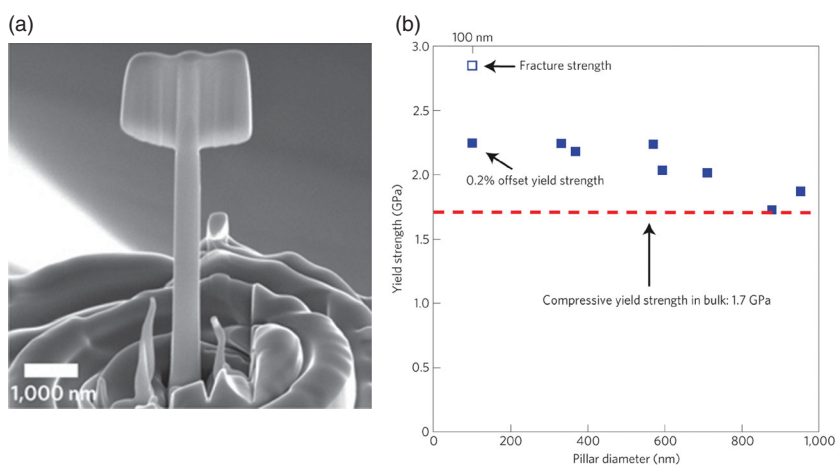

Figure 4. (Colour online) (a) SEM image of a tensile sample. (b)Tensile yield strength as a function of sample diameter.[15]

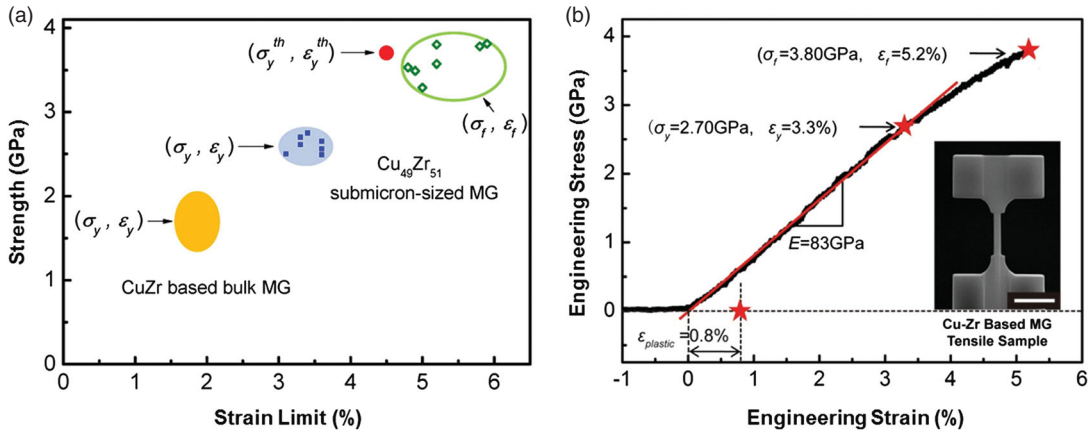

Figure 5. (Colour online) (a) Strength and strain limit of bulk and submicron-sized Cu-Zr MGs. (b) Engineering stress–strain curve from the tension test. The average strain rate was about $2 \times 10^{-3}\,s^{-1}$. Mechanical properties extracted from the stress–strain curve include Young's modulus (E), σ_y and ε_y (defined at the proportionality limit), fracture strength (σ_f) and total elongation to failure (ε_f), as well as the plastic strain ($\varepsilon_{plastic}$) remained in the gauge length. The inset is SEM image of the tensile sample. The scale bar represents 1 μm.[11]

tensile tests of micronanoscaled samples. By creatively using the e-beam-assisted carbon deposition, Tian et al. successfully fabricated tiny carbon markers on their samples, which enabled them to track and measure the strain with very high accuracy while at the same time avoid affecting the intrinsic properties of the samples. Compared to SEM, TEM has higher spatial resolution, which is essential for acquiring accurate strain data. In the size range of 200–300 nm, Tian et al. found that the elastic strain limit and the corresponding strength of submicron-sized MG specimens are about twice as high as the already very impressive elastic limit observed in bulk MG samples (Figure 5(a)). Figure 5(b) is a typical result of a tensile test. Almost all the key parameters (including Young's modulus, proportional limit for both strain and stress, fracture stress) can be deduced by combining the tensile curve and the recorded sample gauge length evolution. It is worth noting that even though the majority of the deformation prior to the fracture is elastic, small amount residual plastic strain (0.8%) was also confirmed in the gauge section.

The gap between the strength of bulk and small volume MGs can be rationalized by considering the shear banding process. Since there are always unavoidable imperfections in bulk samples, the strength is governed by the heterogeneous nucleation of shear bands at the strain concentrators such as casting pores/flaws and surface notches.[34] In the micronanoscaled MG sample, the chances of having a flawless sample largely increase due to the limited volume in the sample. Therefore the nucleation of shear bands in MGs will change from heterogeneous to homogeneous.[34,36,37] Below glass transition temperature T_g, the shear stress required for the homogeneous nucleation of shear bands (upper line in Figure 6) is always higher than that for heterogeneous nucleation (lower line in Figure 6). For given

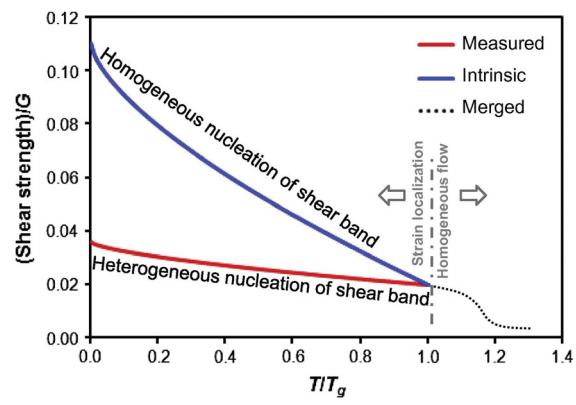

Figure 6. (Colour online) Schematic showing the merging of intrinsic strength and measured strength at Tg for a strain rate of $10^{-3}\,s^{-1}$. The space between the two curves is the strength that can possibly be reached by suppressing the heterogeneous nucleation of shear bands.[34]

temperature, the ideal elastic limit of certain MGs can be estimated based on the homogeneous nucleation of shear bands.[34] The great agreement between the theoretical predication and the experimental measurement demonstrated that the elastic limit of submicron Cu-Zr MG is indeed achieved for the given sample dimensions and loading conditions [11].

It is a remarkable fact that the size-effect on strength in micronanoscaled MGs (only about twice larger) is quite weak compared to that in crystal materials (10–100 times).[38–40] This is probably because the strength of bulk MG is already very high compared to their crystalline counterparts. Consequently, the gap between the bulk value and ideal elastic limit is pretty narrow so that the increase in strength may not obvious. In addition, it is highly expected that the strength–size relationship will

appear different in MGs with different composite, initial condition (thermal history) and different size range.

Plasticity It has been well established experimentally that most bulk MGs fracture in a brittle manner and exhibit little plasticity. However, it was found that for micronanoscaled MGs, not only the yield strength is size aware, so is the deformation mechanism. Shear banding is suppressed and homogeneous deformation is prevalent when sample size is reduced to submicron and nanoscale.

Volkert et al. [14] first reported that once the sample size was below ~400 nm, considerable plastic deformation will be observed for MG pillars under compression tests. As can be seen from Figure 7(a), for the pillar with its diameter of 3.6 μm, numerous shear bands were observed after the compression tests. However, for the pillar with its size of 140 nm, a smooth mushroom postmortem deformation morphology is observed (Figure 7(b). This size-related deformation behavior change was attributed to a required critical strained volume for shear band formation. Similar phenomena were reported by several other research groups.[14,23,24,26,41–43] However, because all these studies were conducted using *ex situ* techniques and people could only examine the samples before and after the tests, the dynamic deformation process remains elusive. In order to solve this puzzle, Shan et al. [35] first carried out compression tests of MG pillars inside a TEM by employing a state-of-the-art *in situ* TEM deformation device (Hysitron PI95 TEM holder [44,45]). It was found that when the diamond flat punch was pushed against the Cu-Zr-Al MG pillar sample, the MG began to flow from the contact interface toward the root parts. Two typical snapshots extracted from the recorded video are shown Figure 7(c)–(d). Obviously, for pillars with smaller enough size, the Cu-Zr-Al MG exhibited very good plastic deformability. Similar phenomena were reported later in other works [10,22,28–32] However, a close examination on these works is ready to find that all the tested samples had a tapered geometry which will undoubtedly generate stress/strain gradient with their magnitude determined by the taper angle and the initial top diameter.[45] Therefore, it had been argued that the observed plastic behavior of MGs during the compression tests might stem from the tapered sample geometry and the imperfect contact interface.

In order to clarify if micronanoscaled MGs are intrinsic ductile or the observed plastic behavior is simply an artifact resulting from the experimental setup, Guo et al. [46] conducted confined tensile tests on nanoscaled MG inside a TEM. As shown in Figure 8(a) and 8(b), the sample experienced obvious necking prior to the final fracture with the total elongation reaching 23%, a typical characteristic of ductile deformation. Based on their observation, the authors concluded that at least submicron-sized MGs can deform in a ductile manner. In addition, in order to convince the readers, the *in situ* TEM compression testing results by Shan et al. [35] (not published at that time) was heavily cited by Guo et al. [46] in their paper. However, their conclusion was still questioned because of the existence of the surrounding frame which has been suspected to be able to suppress the sudden failure of the samples. Such debates continued till the publication by Jang and Greer.[15] By carrying out tensile tests on free-standing MG samples inside SEM, they demonstrated that even without the confined frame, nanoscale MG subjected to uniaxial loading can still experience significant necking behavior, as shown in Figure 8(c)–(e). Similar phenomena were later confirmed by Tian et al. [12] through carrying out quantitative uniaxial tensile tests on MG samples as small as 80 nm inside a TEM, as shown in Figure 9(a)–(h). The corresponding engineering stress vs. strain (Figure 9(h)) demonstrated that at the strain of about 3.2%, the stress and strain curve begin to deviate from linear relationship and localized plastic deformation can be barely seen when the strain reached about 4.6% (Figure 9(c)). Following this, the stress was seen to drop obviously (Figure 9(h)) accompanied by the elegant necking evolution (Figure 9(d)–(f)), which indicates little strain hardening mechanism at play for MGs. After the fracture, the sample showed cup–cone geometry (Figure 9(i)) without any indication

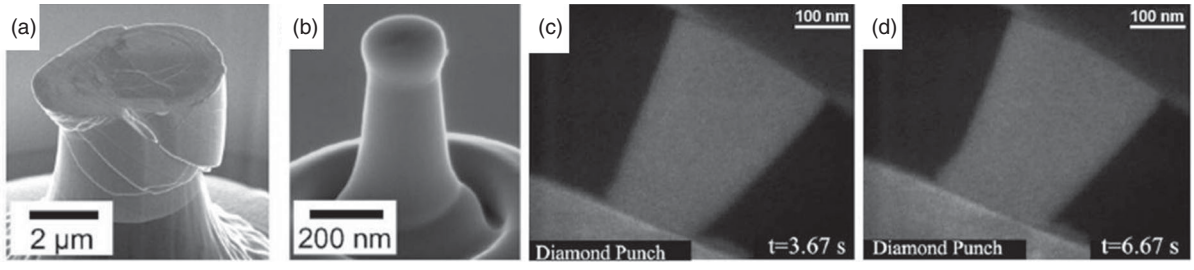

Figure 7. SEM images of deformed (a) 3.61 μm, (b) 140 nm diameter columns.[14] The deformation mechanism changes from shear band formation to homogeneous deformation with decreasing column diameter. (c)–(d) *In situ* dark-field TEM observation of the compression of a MG pillar. Due to the tapered geometry, the plastic deformation was gradually driven down from the top (contact interface) of the pillar (d).[35]

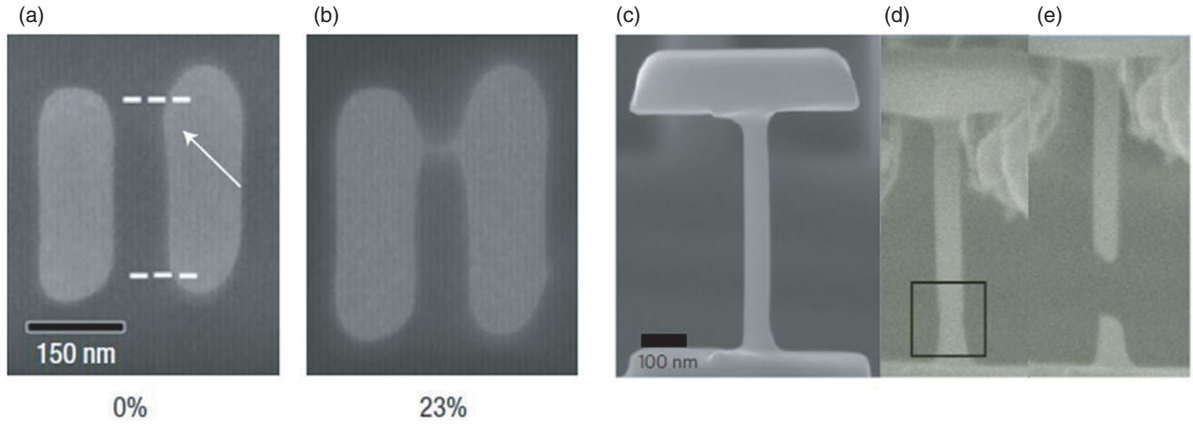

Figure 8. (a)–(b) The virgin tensile sample and the fractured sample with strain to failure of 23%, and the area reduction ratio at fracture as high as ∼80%.[46] (c)–(e) Snapshots of the tensile process of a free-standing sample.[15]

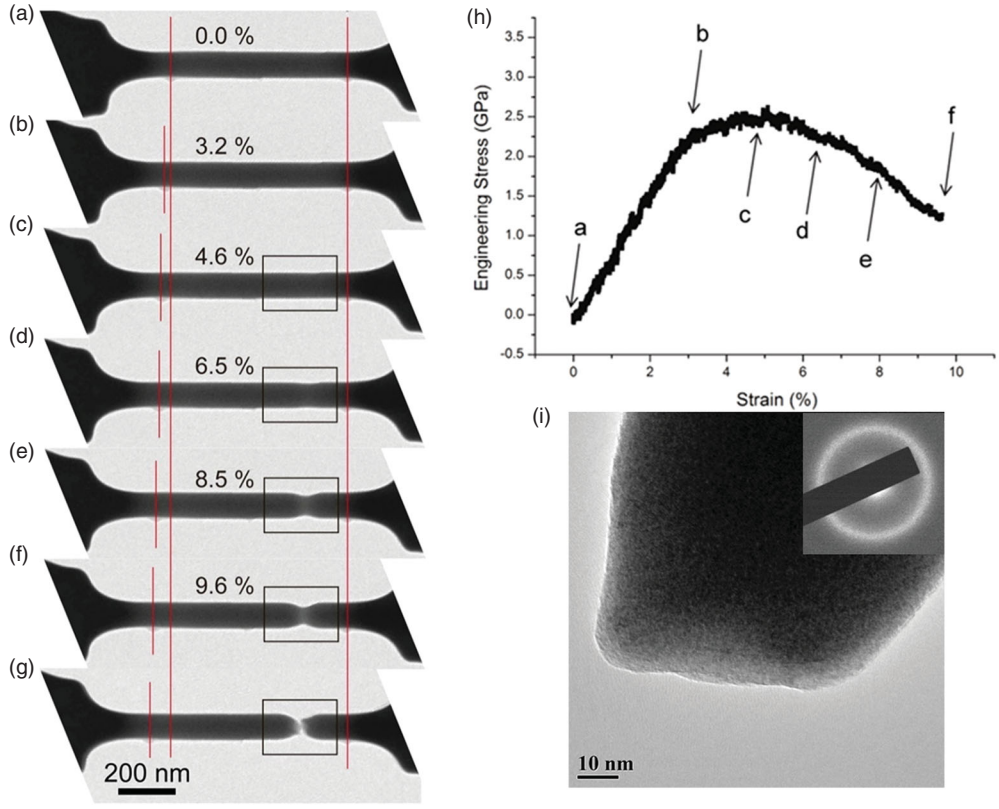

Figure 9. Typical necking process observed during the tensile test of a sample with $D = 80$ nm. (a)–(g) Still frames extracted from the recorded movie. (h) Engineering stress strain curve of this sample. (i) Magnified image of the fractured surface. The inset is the selected area diffraction pattern of the fractured surface. There is no indication of crystallization.

for crystallization (inset in Figure 9(i)) for as-tested samples.

With the reducing sample size, it has been argued that the increased surface-to-volume ratio will increase the total energy of the samples. Consequently, the deformation participation rate [47,48] of the atoms of nanoscale samples will be larger than that of relaxed bulk MGs. This will in turn promote the homogeneous deformation in small-sized samples. However, statistical analysis found that the critical size for the deformation mode transition, that is, from brittle to ductile in MGs, can be affected by many factors, such as sample composition, loading conditions and thermal history. As summarized in Table 2, even though most of the tested MGs exhibit brittle–ductile transition, there are still only a few that exhibit brittle behavior for the tested size range. $Pd_{77}Si_{23}$ MG has the largest transition size so far, reaching a value of ∼400 nm.[14] However, Wang et al.

[22] found that under tension condition, Al-based MG still behaved in a brittle manner even though the sample size is ∼ 100 nm.

Tian et al. [12] are the first to report the strain rate effect on the deformation behavior of nanoscale MG samples. They found that small strain rate can facilitate the necking behavior of MG samples with their size around 80 nm. Figure 10 is a spectrum of fractured surfaces resulted from different strain rate. As can be seen, when the strain rate increased from $0.5 \times 10^{-3}\,s^{-1}$ to about $2.0 \times 10^{-3}\,s^{-1}$, the deformation behavior of as-studied samples will gradually change from necking to shear band. Deformation through shear band will take over for further increased strain rate. It is worth noting that the variation range of the strain rate is less than four times for the complete transition of the deformation mode. This is in sharp contrast with those observed in crystalline materials, which usually need a few orders difference of the strain rate to see the deformation mechanism transition. Presumably, the observed strain rate

Table 2. Various MGs' critical size of deformation mode transition.

References	Composition	Loading	Mode transition	Tested size range	Critical size
Shan et al. [35]	$Cu_{46}Zr_{47}Al_7$	Compression	Yes	330 nm	–
Wu et al. [49]	Zr-based	Compression	No	150 nm	–
Schuster et al. [23,24]	$Pd_{40}Ni_{40}P_{20}$	Compression	No	250 nm – 20 μm	–
Chen et al. [21]	Cu-based	Bending	Yes	93 nm – 645 nm	∼ 200 nm
Chen et al. [30]	Cu-based	Compression	Yes	70 nm – 640 nm	∼ 125 nm
Jang et al. [10]	Zr-based	Compression	Yes	100 nm – 1.6 μm	∼ 100 nm
Bharathula et al. [27,28]	Zr-based	Compression	Yes	200 nm – 3.6 μm	∼ 300 nm
Kuzmin et al. [29]	Zr-based	Compression	Yes	90 nm – 600 nm	∼ 150 nm
Volkert et al. [20]	$Pd_{77}Si_{23}$	Compression	Yes	140 nm – 8 μm	∼ 400 nm
Kuzmin et al. [31,32]	Al-based	Compression	Yes	110 nm – 900 nm	∼ 300 nm
Wang et al. [22]	$Al_{88}Fe_7Gd_5$	Compression	Yes	170 nm – 3 μm	∼ 300 nm
Wang et al. [22]	$Al_{88}Fe_7Gd_5$	Tension	No	100 nm – 400 nm	–
Yi et al. [50]	$Pd_{40}Cu_{30}Ni_{10}P_{20}$	Tension	Yes	267 nm – 1.5 μm	∼ 500 nm
Tian et al. [12]	$Cu_{49}Zr_{51}$	Tension	Yes	70 nm – 112 nm	∼ 80 nm
Jang and Greer [15]	Zr-based	Tension	Yes	100 – 875 nm	∼ 100 nm
Guo et al. [46]	Zr-based	Tension	Yes	100 nm	–
Deng et al. [51]	$Cu_{51}Z_{r49}$	Tension	Yes	∼ 200 nm	–
Luo et al. [52]	Al-based	Tension	Yes	< 20 nm	–

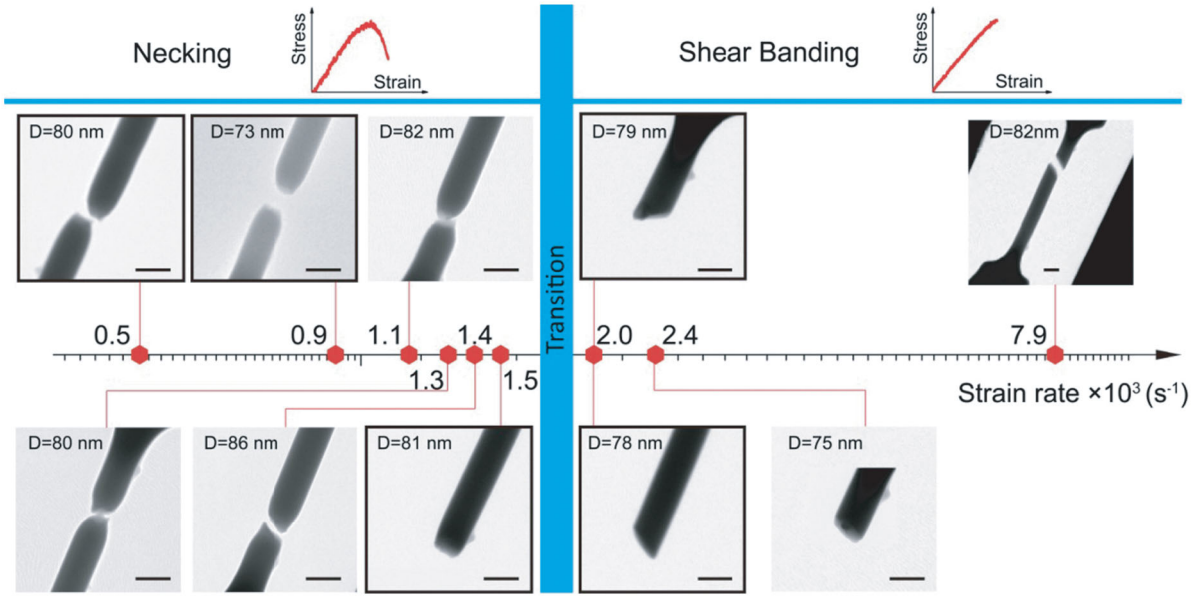

Figure 10. (Colour online) Strain rate effect on deformation mode and fracture morphology. Tensile samples tested with strain rate of 2×10^{-3}/s or higher failed with shear banding, whereas necking occurred when strain rate was lowered to 1.5×10^{-3}/s or less. Although all the 'necking' samples have stress–strain curves featuring gradual stress drop after the peak stress, the morphologies of their fracture surfaces are not identical. Compared with the complete necking features in samples tested with lower strain rate (0.5×10^{-3}/s, 0.9×10^{-3}/s and 1.1×10^{-3}/s), the necking of samples tested at relatively higher strain rate (1.3×10^{-3}/s, 1.4×10^{-3}/s and 1.5×10^{-3}/s) seem to end with shear-like fracture. The scale bars in all the TEM images are 100 nm.[12]

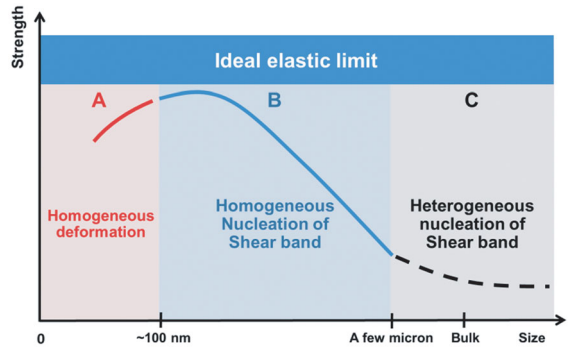

Figure 11. (Colour online) Strength and deformation mechanism of a MG as a function of sample size (adapted from [8]).

dependence is stemmed from the size-dependent diffusion rate change.[53,54] A systematic study on the effect of size and strain rate on the deformation mechanism of micronanoscaled MGs pillars is carried out by Tonnies et al. [55] A size-dependent critical diameter for the deformation mechanism transition is revealed and a size-strain rate deformation map is proposed.

The deformation mechanism and strength of a MG vs. the sample size is summarized in Figure 11.[8] For samples with their size less than 100 nm or so (zone A), with the decreasing sample size, the strength of the MG will decrease because of the increasing influence of the surface diffusion. In zone A, strain-rate-dependent necking behavior will begin to dominate, the participation rate of the atom in the plastic deformation increases gradually and result in significant plasticity. For the samples with their size ranging from $\sim$100 nm to a few micron meter (zone B), the strength of the MG will increase with the decreasing sample size till reaching the theoretical plateau because of the gradually depletion of critical-sized flaws. In zone B, the strength of the MG will be determined by the shear band nucleation. For the sample with their size larger than a few micrometer (zone C), the strength of the MG is almost size-independent and samples always fractured in a brittle manner. In zone C, it is the shear band propagation that control the strength because of the inevitable critical-sized flaws which can reduce the shear band nucleation stress dramatically due to the stress concentration.

Fatigue Properties of Micronanoscaled MGs So far, it has been demonstrated experimentally that micronanoscaled MGs not only impart ultrahigh strength and elastic limit, but also exhibit considerable plastic deformability. This indicates that micronanoscaled MGs may have promising applications in MEMS and NEMS. For instance, TiAl-based MG hinges which allow the rotation of micro-mirrors have been used in a digital light processor.[56] However, in order to have reliable products with great performance, it is necessary to study systematically the fatigue properties of micronanoscaled MGs.

The very first reported research on the fatigue tests of micronanoscaled MG was carried out by Jang et al. [57] They found that in compression–compression fatigue experiments, Zr-based MG pillar with its diameter of 1.6 μm could sustain 40×10^6 cycles under a load of $\sim$2 GPa (110% of bulk yield stress). In contrast, pillars with the same diameter fail immediately at a stress larger than 2 GPa. In bending tests, they found that no pillar fails below 10×10^6 cycles even at 90% of bulk yield stress. Comparing to bulk samples, micronanoscaled MGes have higher fatigue endurance limit and better fatigue resistance. However, it is worth noting that even for samples without catastrophic failure, obvious fatigue damage in terms of small shear band and plastic deformation can still be found at the free end side of the pillars after the fatigue tests. Therefore, it is necessary to study the fatigue damage mechanism of micronanoscaled MGs.

Ye et al. [58] studied micronanoscaled MG pillar samples through cycle loading with different frequency with the aim to probe the microstructure of MGs. They found that at a relatively low stress rate, 1.42 GPa/s, the recorded displacement spectrum synchronized with that of load, similar to that observed in quasi-static tests. However, in high stress/strain rate test, the read out spectra of displacement and load are out of phase and exhibited a mechanical hysteresis loop. Based on above observations, the authors speculated that MG pillars will experience elastic response at low stress/strain rate but will exhibit viscoelastic behavior at high stress/strain rate. Further, the authors proposed a core–shell atomistic model to rationalize the observed phenomena and concluded that the liquid-like deformation of free-volume zones is responsible for the hysteresis of the micropillars under dynamic loading. However, our recent tests on fused silica with same type of instrument found that similar phenomena can also be achieved (Shan group, unpublished work). Detailed analysis suggested that at high loading rate, the instrument itself will generate a rate-dependent shift of the real force and displacement relative to the programed force. Therefore, it remains for discussion if the phenomena observed by Ye et al. is the intrinsic properties of the studied MG or phenomena resulted from the instrument.

Wang et al. [59] were the first to reveal the fatigue damage mechanism of micronanoscaled MG samples inside TEM. They used pre-notched cantilevers to probe the microstructure evolution of an $Al_{88}Fe_7Gd_5$ MG in response to cyclic bending tests. One typical example of such cantilever is shown in Figure 12(a). The notch was quite smooth prior to the cyclic bending tests (Figure 12(b) and 12(c)). However, after 490 cycles, the initial smooth surface of the notch got roughened

(Figure 12(c)–(d)), similar to the extrusion phenomena observed in bulk copper during the fatigue test, but no such phenomena were observed for MG samples subjected to monotonic loading. It was worth noting that unlike that in crystalline materials, there are no long range plastic carriers, for example, dislocations, in MG. Further cyclic loading led to the nucleation and propagation of a crack at the root part of the notch (Figure 12(e)). Interestingly, numerous tiny grains were observed in the crack tip area. The growth and coalescence of these tiny grains during cyclic straining were observed to impede subsequent crack growth by bridging the crack. By the end of 1960 cycles, a few large grains can be clearly identified ahead of the crack tip in the bright-field TEM image (Figure 12(f)) , as was confirmed by the selected area diffraction patterns (inset in Figure 12(f)). With the help of the molecular dynamics simulations, the authors demonstrated that their findings can be rationalized by the accumulations of strain-induced nonaffine atomic rearrangements that effectively enhance diffusion through random walk during repeated strain cycles.

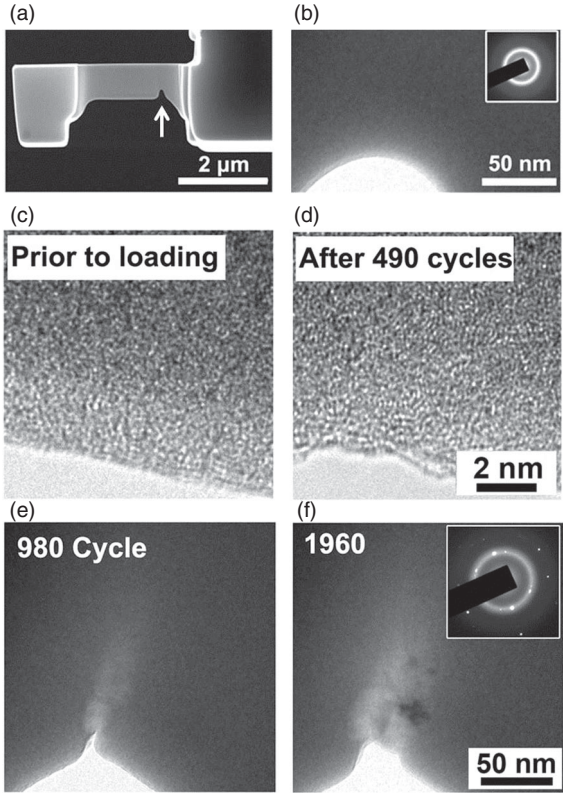

Figure 12. (a) SEM image showing a cantilever fabricated by a FIB. (b) Bright-field TEM image of the notch tip before testing shows that the sample has a fully amorphous structure, as evidenced by the SADP (Inset). (c)–(d) High-magnification images of the notch-tip surface region for the untested and cyclically strained (maximum strain $\sim$2.1%) samples. (e)–(f) Fatigue crack morphology after 980 and 1,960 cycles, respectively. SADP (Inset) demonstrated the existence of crystalline phase ahead of the crack tip [59].

The studies on the fatigue properties and dynamic behavior of micronanoscaled MGs are of great importance regarding the performance and reliability of MG components in micro-and nanoscale systems. Therefore, this field is becoming a research hotspot. These interesting results not only enrich our knowledge on the structure of MGs, but also provide insights on the fundamental damage mechanism of MGs and therefore are very helpful in materials design and engineering applications.

Effects from e-beam and Ion-beam For the studies on micronanoscaled MGs, the majority of the samples were fabricated through FIB and most of the tests were carried out inside SEM or TEM. Therefore, the frequently asked questions are that: what is the effect of ion beam and what is the effect of e-beam on the measured properties? Through *in situ* quantitative TEM compression tests, Wang et al. [60] demonstrated that with and without the illumination of an e-beam, the flow stress of amorphous silica spheres can be changed from 2.5 to 10 GPa. At the same time, the plastic deformability of silica spheres can be improved dramatically by the e-beam. Further studies (Shan's group, unpublished work) found that under normal illustration conditions, e-beam has no obvious effect on the mechanical properties of materials with metallic bond, but may have a dramatic effect on the mechanical behavior of materials with ionic or covalent bonds. Tian et al. [12] studied the e-beam effect on deformation behavior of MG samples. They carried out comparative trials on samples with the same diameter of 80 nm to address the possible e-beam effect by switching on and off the e-beam. They found that in both cases, the samples failed with ductile necking and no obvious difference was identified between the samples tested under normal illumination condition and those tested without e-beam. This simply suggested that e-beam irradiation should not play a key role for the observed tensile ductility of MGs.[12,46,52] However, Tian et al. [12] also found that excessively intense e-beam (orders higher in density compared with those under normal testing conditions) could result in obvious plastic deformation behavior in much larger samples (e.g. 130 nm) since it could possibly increase sample temperature or enhance sputtering and atom displacement.

FIB milling is an effective method to fabricate micronanoscaled samples and has been wildly used in the study of mechanical behavior of micronanoscaled materials. The FIBed samples are subjected to high energy Ga+ bombardment. Therefore, the microstructure of FIBed samples may be changed during fabrication process. For MGs, FIB milling can introduce free volume or chemical softening, and result in heavily disordered glass structure.[61] The appealing ductility in FIBed MG samples could be related to these

changes. Therefore, it is necessary to study the FIB effect. Magagnosc et al. [62] fabricated MG nanowires with diameters ranging from 50 to 200 nm by thermoplastic molding. They compared the mechanical behavior of nanowires irradiated by Ga+ with as molded nanowires. The results showed Ga+ irradiation could increase plasticity of the nanowires and further annealing turned the samples back to brittleness. However, by conducting tensile tests on nanoscale MG tensile samples fabricated by electroplating, Jang et al. [63] found that FIB free samples also display certain plasticity. These results suggest the observed ductile behavior may be the intrinsic properties of micronanoscaled MGs. The fact that different processing methods, such that FIB cutting and electroplating FIB processing, can lead very different mechanical behavior of micronanoscaled MGs can be rationalized as below: the processing routes can modify the structure, especially surface structure in materials, and therefore result in MGs with different potential energies, which in turn result in different mechanical behavior. To verify this speculation, it is of great importance to study the subtle changes in MG structure and quantify energy states in MGs produced in different ways.

Conclusions and Outlook Past decade has witnessed profound progress in experimental methods and techniques, which enable us to explore the micronanoscaled world, that we could not reach before. The state-of-the-art mechanical tests demonstrated that micronanoscaled MGs are in general stronger and more ductile than their bulk counterparts. Combined with theoretical calculations and computer simulations, a deformation mechanism map with multiple dimensions on MGs has been achieved, which is expected to provide guidance for the design and application of micronanoscaled MGs. However, there are still several unsettled problems that need scientific and technological endeavors, including: (1) it remains a puzzle experimentally on the local atomic structure of the MGs and its dynamic evolution in response to applied stress. New characterization devices with high spatial and time resolution and low interference with the probing materials are necessary to solve this puzzle. (2) The nature of STZ and free volume and their link with shear band. Even though STZ has been widely cited as the dominant plastic carrier for MGs, experimentally no one has imaged a STZ so far. Consequently, the concept of STZ or free volume need to be re-evaluated and improved to make it as physically acceptable as dislocation in crystalline materials. (3) Life evaluation method of micronanoscaled MGs. So far, only very limited data available on the fatigue properties of micronanoscaled MGs under the action of cyclic force/stress. In order to make these promising materials into reliable and durable devices, it is necessary to study symmetrically the fatigue properties of micronanoscaled MGs under the effect of multi-field coupling conditions, such as thermo-electrical, thermo-mechanical or electrical–mechanical.

Disclosure statement No potential conflict of interest was reported by the authors.

Funding This work was supported by the grants from NSFC [51231005, 51471128, 51321003, and 51501144] and 973 Program of China [2012CB619402]. We also appreciate the support from the 111 Project of China [B06025] and China Postdoctoral Science Foundation [2015M580842].

References

[1] Chaudhari P, Turnbull D. Structure and properties of metallic glasses. Science. 1978;199(4324):11–21.
[2] Greer AL. Metallic glasses . . . on the threshold. Mater Today. 2009;12(1–2):14–22.
[3] Cheng YQ, Ma E. Atomic-level structure and structure-property relationship in metallic glasses. Prog Mater Sci. 2011;56(4):379–473.
[4] Ashby M, Greer A. Metallic glasses as structural materials. Scripta Mater. 2006;54(3):321–326.
[5] Schuh CA, Hufnagel TC, Ramamurty U. Mechanical behavior of amorphous alloys. Acta Mater. 2007;55(12): 4067–4109.
[6] Wang WH. The elastic properties, elastic models and elastic perspectives of metallic glasses. Prog Mater Sci. 2012;57(3):487–656.
[7] Schroers J. Bulk metallic glasses. Phys Today. 2013;66(2): 32–37.
[8] Greer AL, Cheng YQ, Ma E. Shear bands in metallic glasses. Mater Sci Eng, R. 2013;74(4):71–132.
[9] Johnson W, Samwer K. A Universal Criterion for plastic yielding of metallic glasses with a $(T/T_g)^{2/3}$ temperature dependence. Phys Rev Lett. 2005;95(19:1–4).
[10] Jang D, Gross CT, Greer JR. Effects of size on the strength and deformation mechanism in Zr-based metallic glasses. Int J Plast. 2011;27(6):858–867.
[11] Tian L, Cheng YQ, Shan ZW, Li J, Wang CC, Han XD, Sun J, Ma E. Approaching the ideal elastic limit of metallic glasses. Nat Commun. 2012;3(609):1–6.
[12] Tian L, Shan Z-W, Ma E. Ductile necking behavior of nanoscale metallic glasses under uniaxial tension at room temperature. Acta Mater. 2013;61(13):4823–4830.
[13] Shan Z. In situ TEM investigation of the mechanical behavior of micronanoscaled metal pillars. Jom. 2012;64(10):1229–1234.
[14] Volkert CA, Donohue A, Spaepen F. Effect of sample size on deformation in amorphous metals. J Appl Phys. 2008;103(8):083539.
[15] Jang DC, Greer JR. Transition from a strong-yet-brittle to a stronger-and-ductile state by size reduction of metallic glasses. Nat Mater. 2010;9(3):215–219.
[16] Yavari AR, Georgarakis K, Botta WJ, Inoue A, Vaughan G. Homogenization of plastic deformation in metallic glass foils less than one micrometer thick. Phys Rev B. 2010;82(17):1–4.
[17] Dubach A, Raghavan R, Loffler J, Michler J, Ramamurty U. Micropillar compression studies on a bulk metallic glass in different structural states. Scripta Mater. 2009;60(7):567–570.

[18] Yang Y, Ye JC, Lu J, Liu CT. Dual character of stable shear banding in bulk metallic glasses. Intermetallics. 2011;19(7):1005–1013.

[19] Yang Y, Ye JC, Lu J, Liaw PK, Liu CT. Characteristic length scales governing plasticity/brittleness of bulk metallic glasses at ambient temperature. Appl Phys Lett. 2010;96(1):011905.

[20] Ye JC, Lu J, Yang Y, Liaw PK. Extraction of bulk metallic-glass yield strengths using tapered micropillars in micro-compression experiments. Intermetallics. 2010;18(3):385–393.

[21] Chen CQ, Pei YT, De Hosson JTM. Effects of size on the mechanical response of metallic glasses investigated through in situ TEM bending and compression experiments. Acta Mater. 2010;58(1):189–200.

[22] Wang CC, Ding J, Cheng YQ, Wan JC, Tian L, Sun J, Shan Z.-W., Li J, Ma E. Sample size matters for Al88Fe7Gd5 metallic glass: smaller is stronger. Acta Mater. 2012;60(13–14):5370–5379.

[23] Schuster BE, Wei Q, Ervin MH, Hruszkewycz SO, Miller MK, Hufnagel TC, Ramesh KT. Bulk and microscale compressive properties of a Pd-based metallic glass. Scripta Mater. 2007;57(6):517–520.

[24] Schuster BE, Wei Q, Hufnagel TC, Ramesh KT. Size-independent strength and deformation mode in compression of a Pd-based metallic glass. Acta Mater. 2008;56(18):5091–5100.

[25] Wang YB, Lee CC, Yi J, An XH, Pan MX, Xie KY, Liao XZ, Cairney JM, Ringer SP, Wang WH. Ultrahigh-strength submicron-sized metallic glass wires. Scripta Mater. 2014;84–85:27–30.

[26] Lai YH, Lee CJ, Cheng YT, Chou HS, Chen HM, Du XH, Chang CI, Huang JC, Jian SR, Jang JSC, Nieh TG. Bulk and microscale compressive behavior of a Zr-based metallic glass. Scripta Mater. 2008;58(10):890–893.

[27] Bharathula A, Flores KM. Variability in the yield strength of a metallic glass at micron and submicron length scales. Acta Mater. 2011;59(19):7199–7205.

[28] Bharathula A, Lee S-W, Wright WJ, Flores KM. Compression testing of metallic glass at small length scales: effects on deformation mode and stability. Acta Mater. 2010;58(17):5789–5796.

[29] Kuzmin OV, Pei YT, De Hosson JTM. In situ compression study of taper-free metallic glass nanopillars. Appl Phys Lett. 2011;98(23):233104.

[30] Chen CQ, Pei YT, Kuzmin O, Zhang ZF, Ma E, De Hosson JTM. Intrinsic size effects in the mechanical response of taper-free nanopillars of metallic glass. Phys Rev B. 2011;83(18):1–4.

[31] Kuzmin OV, Pei YT, De Hosson JTM. Size effects and ductility of Al-based metallic glass. Scripta Mater. 2012;67(4):344–347.

[32] Kuzmin OV, Pei YT, Chen CQ, De Hosson JTM. Intrinsic and extrinsic size effects in the deformation of metallic glass nanopillars. Acta Mater. 2012;60(3):889–898.

[33] Telford M. The case for bulk metallic glass. Mater Today. 2004;7(3):36–43.

[34] Cheng YQ, Ma E. Intrinsic shear strength of metallic glass. Acta Mater. 2011;59(4):1800–1807.

[35] Shan ZW, Li J, Cheng YQ, Minor AM, Syed Asif SA, Warren OL, et al. Plastic flow and failure resistance of metallic glass: insight from in situ compression of nanopillars. Phys Rev B. 2008;77(15):1–6.

[36] Jiang MQ, Jiang F, Keryvin V, Meng JX, Sun J, Dai LH. Relation between ideal and real strengths of metallic glasses. J Non-Cryst Solid. 2012;358(23):3119–3123.

[37] Yang Y, Liu CT. Size effect on stability of shear-band propagation in bulk metallic glasses: an overview. J Mater Sci. 2012;47(1):55–67.

[38] Greer JR, De Hosson JTM. Plasticity in small-sized metallic systems: intrinsic versus extrinsic size effect. Prog Mater Sci. 2011;56(6):654–724.

[39] Uchic MD, Dimiduk DM, Florando JN, Nix WD. Sample dimensions influence strength and crystal plasticity. Science. 2004;305(5686):986–989.

[40] Brenner SS. Tensile strength of whiskers. J Appl Phys. 1956;27(12):1484–91.

[41] Cheng S, Wang X-L, Choo H, Liaw PK. Global melting of Zr57Ti5Ni8Cu20Al10 bulk metallic glass under microcompression. Appl Phys Lett. 2007;91(20):201917-1–3.

[42] Lee CJ, Huang JC, Nieh TG. Sample size effect and microcompression of Mg65Cu25Gd10 metallic glass. Appl Phys Lett. 2007;91(16):161913-1–3.

[43] Zheng Q, Cheng S, Strader JH, Ma E, Xu J. Critical size and strength of the best bulk metallic glass former in the Mg–Cu–Gd ternary system. Scripta Mater. 2007;56(2):161–164.

[44] Minor AM, Asif SA, Shan ZW, Stach EA, Cyrankowski E, Wyrobek TJ, Warren OL. A new view of the onset of plasticity during the nanoindentation of aluminium. Nat Mater. 2006;5(9):697–702.

[45] Shan ZW, Mishra RK, Asif SA, Warren OL, Minor AM. Mechanical annealing and source-limited deformation in submicrometre-diameter Ni crystals. Nat Mater. 2008;7(2):115–119.

[46] Guo H, Yan PF, Wang YB, Tan J, Zhang ZF, Sui ML, Ma E. Tensile ductility and necking of metallic glass. Nat Mater. 2007;6(10):735–739.

[47] Shi Y, Falk M. Strain Localization and Percolation of Stable Structure in Amorphous Solids. Phys Rev Lett. 2005;95(9):1–4.

[48] Shi Y, Falk M. Atomic-scale simulations of strain localization in three-dimensional model amorphous solids. Phys Rev B. 2006;73(21):1–10.

[49] Wu XL, Guo YZ, Wei Q, Wang WH. Prevalence of shear banding in compression of $Zr_{41}Ti_{14}Cu_{12.5}Ni_{10}Be_{22.5}$ pillars as small as 150nm in diameter. Acta Mater. 2009;57(12):3562–3571.

[50] Yi J, Wang WH, Lewandowski JJ. Sample size and preparation effects on the tensile ductility of Pd-based metallic glass nanowires. Acta Mater. 2015;87:1–7.

[51] Deng Q, Cheng Y, Yue Y, Zhang L, Zhang Z, Han X, Ma E. Uniform tensile elongation in framed submicron metallic glass specimen in the limit of suppressed shear banding. Acta Mater. 2011;59(17):6511–6518.

[52] Luo JH, Wu FF, Huang JY, Wang JQ, Mao SX. Superelongation and atomic chain formation in nanosized metallic glass. Phys Rev Lett. 2010;104(21):1–4.

[53] Tian L, Li J, Sun J, Ma E, Shan ZW. Visualizing size-dependent deformation mechanism transition in Sn. Sci Rep. 2013;3(2113):1–6.

[54] Sun J, He L, Lo Y-C, Xu T, Bi H, Sun L, Zhang Z, Mao SX, Li J. Liquid-like pseudoelasticity of sub-10-nm crystalline silver particles. Nat Mater. 2014;13(11):1007–1012.

[55] Tonnies D, Maass R, Volkert CA. Room temperature homogeneous ductility of micrometer-sized metallic glass. Adv Mater. 2014;26(32):5715–5721.

[56] Tregilgas JH. Amorphous titanium aluminide hinge. Adv Mater Process. 2004;162(10):40–41.

[57] Jang D, Maaß R, Wang G, Liaw PK, Greer JR. Fatigue deformation of microsized metallic glasses. Scripta Mater. 2013;68(10):773–776.
[58] Ye JC, Lu J, Liu CT, Wang Q, Yang Y. Atomistic free-volume zones and inelastic deformation of metallic glasses. Nat Mater. 2010;9(8):619–623.
[59] Wang CC, Mao YW, Shan ZW, Dao M, Li J, Sun J, Ma E, Suresh S. Real-time, high-resolution study of nanocrystallization and fatigue cracking in a cyclically strained metallic glass. PNAS. 2013;110(49):19725–19730.
[60] Zheng K, Wang C, Cheng Y-Q, Yue Y, Han X, Zhang Z, Shan Z, Mao SX, Ye M, Yin Y, Ma E. Electron-beam-assisted superplastic shaping of nanoscale amorphous silica. Nat Commun. 2010;1(3):1–8.
[61] Liu YH, Zhao F, Li YL, Chen MW. Deformation behavior of metallic glass thin films. J Appl Phys. 2012;112(6):063504.
[62] Magagnosc DJ, Ehrbar R, Kumar G, He MR, Schroers J, Gianola DS. Tunable tensile ductility in metallic glasses. Sci Rep. 2013;3(1096):1–6.
[63] Chen DZ, Jang D, Guan KM, An Q, Goddard WA, 3rd, Greer JR. Nanometallic glasses: size reduction brings ductility, surface state drives its extent. Nano Lett. 2013;13(9):4462–4468.